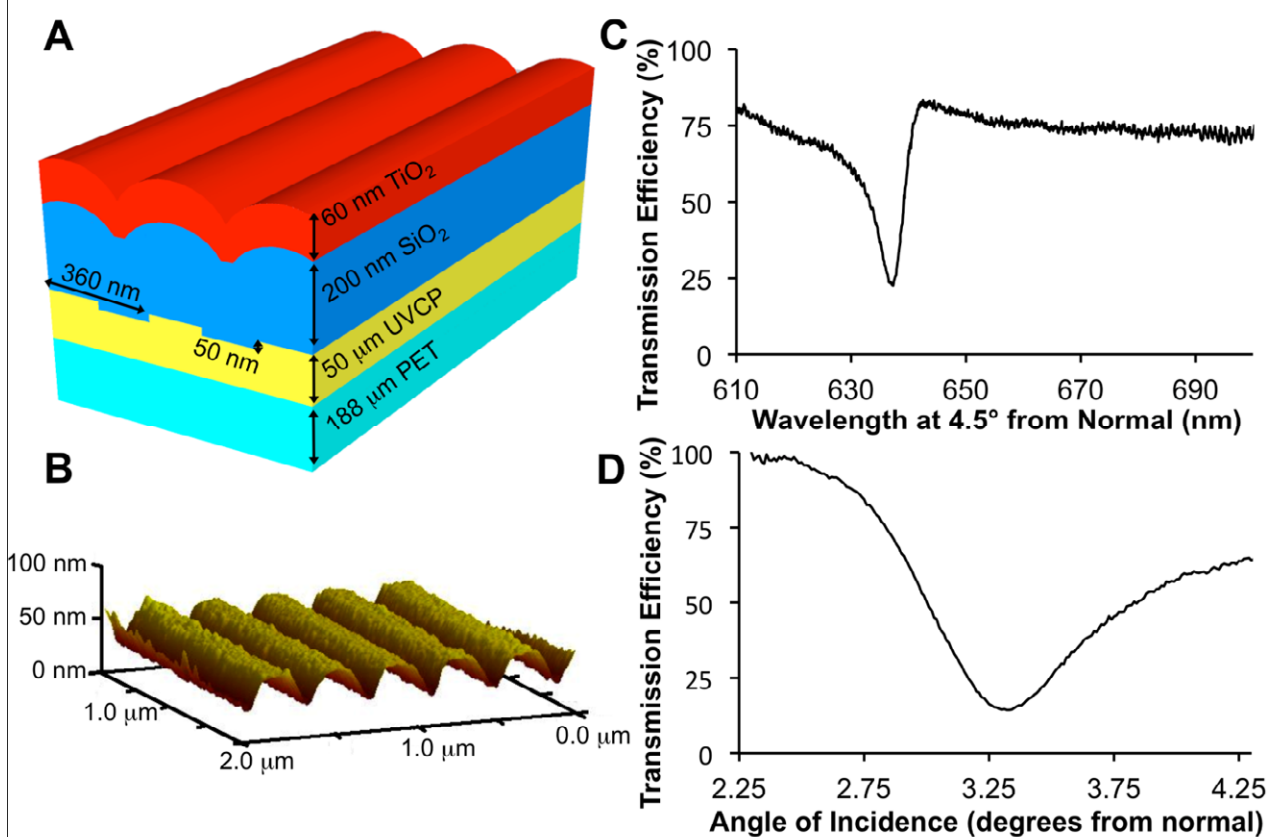
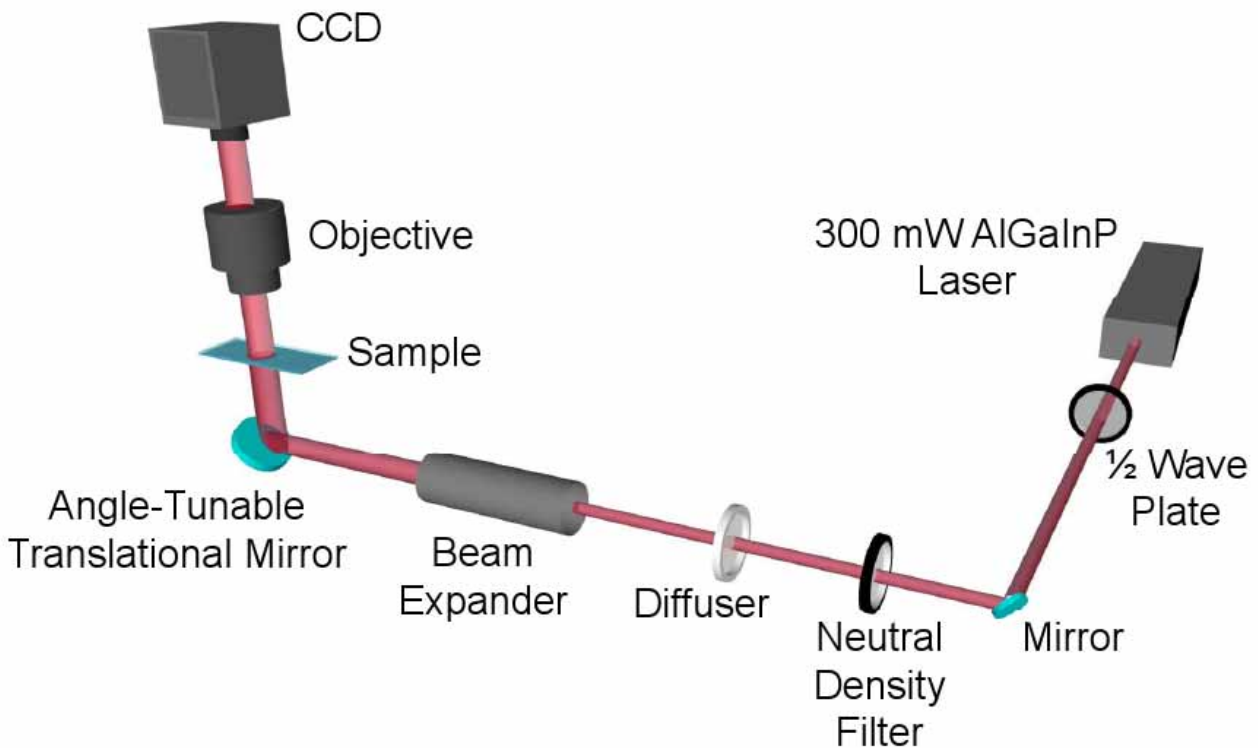


**Supplementary Figure 1**



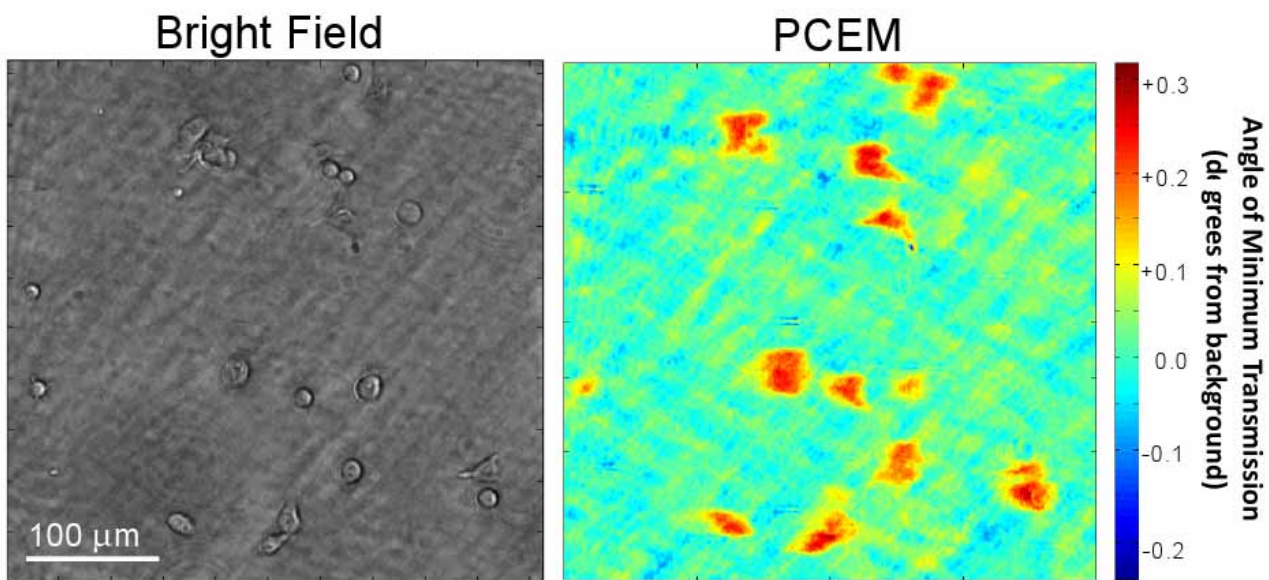
Supplementary Figure 1: a) Schematic illustration of the PC biosensor configuration. A photoreplica molding process yields a grating pattern composed of UV-curable polymer (UVCP), which is affixed to a layer of polyethylene terephthalate (PET). The resulting grating is then coated with SiO<sub>2</sub> and TiO<sub>2</sub> to complete fabrication. b) Atomic force microscopy (AFM) image of a PC biosensor. c) PC biosensor characterization by wavelength. The resonant wavelength of a PC biosensor is rejected by the biosensor structure, resulting in decreased transmission efficiency. d) PC biosensor characterization by angle of incidence. The resonant angle of incidence in combination with the illumination using the resonant wavelength results in satisfaction of the resonant condition of the PC biosensor, resulting in decreased transmission efficiency.

**Supplementary Figure 2**



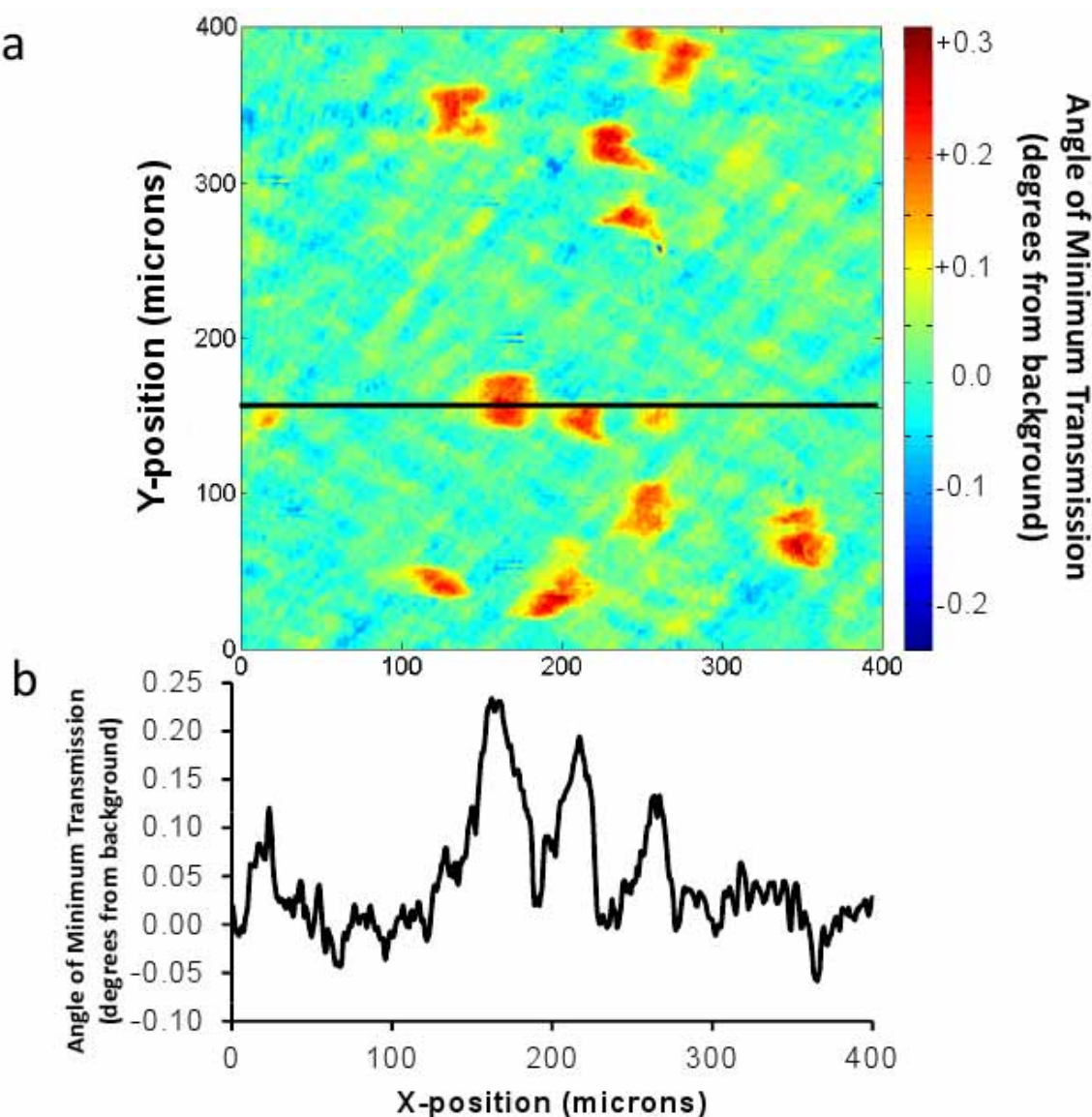
Supplementary Figure 2: Schematic depiction of the photonic crystal enhanced microscope. Collimated 637 nm light emitted from a diode laser is directed into a  $\frac{1}{2}$  wave-plate for control of polarization before being attenuated by a variable neutral density filter. The beam is then directed through a diffuser and into a beam expander to provide a broadly uniform illumination source. The angle of incidence upon the sample is controlled by an angle-tunable mirror mounted on a translational stage. Transmitted light is magnified and focused by an objective lens and recorded by a CCD.

**Supplementary Figure 3**



Supplementary Figure 3: Wide-field capability of PCEM. PCEM imaging allows simultaneous label-free and bright field imaging of cell attachment over wide areas. At 20x magnification, the field of view encompasses an area of  $0.16\text{ mm}^2$ .

**Supplementary Figure 4**



Supplementary Figure 4: PCEM Line Plot. HepG2/C3 hepatic carcinoma cells cultured for 2h show significantly increased attachment protein density, as indicated by PCEM (a) and a line plot taken across the AMT profiles of three cells (b).

Supplementary Table 1: Data recorded for evaluation of cardiac myocytes in culture on PC biosensors coated with fibronectin and collagen, as well as for cardiac myocytes in culture on uncoated PC biosensors.

Cell	ECM Coating	AMT Shift (degrees from background)	Standard Deviation	Contractility	Spreading
1	fibronectin, collagen	0.181	0.026	+	+
2	fibronectin, collagen	0.168	0.011	+	+
3	fibronectin, collagen	0.215	0.037	+	+
4	fibronectin, collagen	0.224	0.024	+	+
5	fibronectin, collagen	0.276	0.023	+	+
6	fibronectin, collagen	0.134	0.011	+	+
7	fibronectin, collagen	0.008	0.014	-	-
8	fibronectin, collagen	0.011	0.024	-	-
9	fibronectin, collagen	0.113	0.026	+	+
10	uncoated	0.161	0.026	-	+
11	uncoated	0.181	0.131	-	+
12	uncoated	0.143	0.017	-	+
13	uncoated	0.010	0.024	-	-
14	uncoated	0.109	0.021	-	+
15	uncoated	0.020	0.011	-	-
16	uncoated	0.185	0.019	-	+
17	uncoated	0.096	0.018	-	+
18	uncoated	0.059	0.014	-	-
19	uncoated	0.033	0.033	-	-
20	uncoated	0.022	0.025	-	-
21	uncoated	0.040	0.018	-	-
22	uncoated	0.052	0.016	-	-
23	uncoated	0.071	0.009	-	-
24	uncoated	0.058	0.016	-	-